ifet-1 is a broad-scale translational repressor required for normal P granule formation in *C. elegans*

Madhu S. Sengupta[1], Wai Yee Low[1], Joseph R. Patterson[2], Hyun-Min Kim[3], Ana Traven[1], Traude H. Beilharz[1], Monica P. Colaiácovo[2], Jennifer A. Schisa[2] and Peter R. Boag[1],*

[1]Department of Biochemistry and Molecular Biology, Monash University, Victoria 3800, Australia
[2]Department of Biology, Central Michigan University, Mount Pleasant, MI 48859, USA
[3]Department of Genetics, Harvard Medical School, MA 02115, USA

*Author for correspondence (peter.boag@monash.edu)

Summary

Large cytoplasmic ribonucleoprotein germ granule complexes are a common feature in germ cells. In *C. elegans* these are called P granules and for much of the life-cycle they associate with nuclear pore complexes in germ cells. P granules are rich in proteins that function in diverse RNA pathways. Here we report that the *C. elegans* homolog of the eIF4E-transporter IFET-1 is required for oogenesis but not spermatogenesis. We show that IFET-1 is required for translational repression of several maternal mRNAs in the distal gonad and functions in conjunction with the broad-scale translational regulators CGH-1, CAR-1 and PATR-1 to regulate germ cell sex determination. Furthermore we have found that IFET-1 localizes to P granules throughout the gonad and in the germ cell lineage in the embryo. Interestingly, IFET-1 is required for the normal ultrastructure of P granules and for the localization of CGH-1 and CAR-1 to P granules. Our findings suggest that IFET-1 is a key translational regulator and is required for normal P granule formation.

Key words: eIF4E transporter, P granule, Germ granules, Translational regulation, *Caenorhabditis elegans*

Introduction

Germ cells are unique as they are immortal and pluripotent. In all species examined, germ cells contain a distinctive electron dense, non-membranous, cytoplasmic structure called germ granules. Germ granules are highly enriched in RNAs and RNA-binding proteins and are key regulators of RNA metabolism in germ cells (Voronina et al., 2011). The presence of germ granules within germ cells can vary between species, for example in *C. elegans* germ granules are continually present and are required for normal proliferation and differentiation (Kawasaki et al., 1998; Spike et al., 2008). In mammals, germ granules form *de novo* and are present mainly in the later stages of germ cell development (Pepling et al., 2007). Despite this difference, it is clear that germ granules in both invertebrates and vertebrates share many of the same proteins and likely play similar functions in regulating multiple RNA pathways critical for gametogenesis and early embryonic development.

In *C. elegans*, germ granules are known as P granules. For most of the gonad, P granules are located in perinuclear foci tightly associated with the nuclear pore complex (NPC) (Fig. 1A) (Pitt et al., 2000; Schisa et al., 2001) and appear to extend the nuclear pore environment into the cytoplasm (Updike et al., 2011). Recent studies have found that nascent mRNAs are transported through the NPC to perinuclear P granules and that transcription is required for the localization of two P granule-specific components, PGL-1, the P granule nucleating factor and eIF4E-binding protein, and GLH-2, the *C. elegans* homolog of the DEAD-box RNA helicase Vasa (Sheth et al., 2010). Although perinuclear P granules are continuously associated with transcriptionally active germ cells, components within these granules appear to be highly dynamic. Fluorescence recovery after photobleaching (FRAP) experiments demonstrated a very rapid recovery of PGL-1::GFP fluorescence in perinuclear P granules (Sheth et al., 2010). In late stage oocytes, where transcription appears to be off, P granules detach from the nuclear pore and become dispersed throughout the cytoplasm (Fig. 1A). Over 40 proteins have now been localized to P granules including proteins involved in Dicer-dependent and Dicer-independent small RNA pathways, and regulators of transcription and translation (Voronina et al., 2011). Interestingly, some P granule components also function in somatic processing (P) bodies where they are important factors in the decapping mediated mRNA turnover pathway (Sheth and Parker, 2003). These include the DEAD box RNA helicase CGH-1 and the Lsm- and RGG-domain containing protein CAR-1, both of which are required for normal levels of germ cell apoptosis and gonad function (Navarro et al., 2001; Audhya et al., 2005; Boag et al., 2005). This has led to the speculation that germ granules and P bodies are evolutionarily related hubs of mRNA regulation in germ and somatic cells, respectively (Strome and Lehmann, 2007).

In P bodies, CGH-1 and CAR-1 homologs function as 'general' translational repressors and activators of mRNA decapping (Coller and Parker, 2005; Nissan et al., 2010). In mammalian cell culture, the CGH-1 homolog RCK directly interacts with the metazoan-specific eIF4E-transporter (4E-T), which is a nuclear/cytoplasmic shuttling protein required for P body formation. Knockdown of 4E-T results in loss of RCK from P bodies, while overexpression of 4E-T leads to inhibition of cap-dependent translation (Andrei et al., 2005; Ferraiuolo et al.,
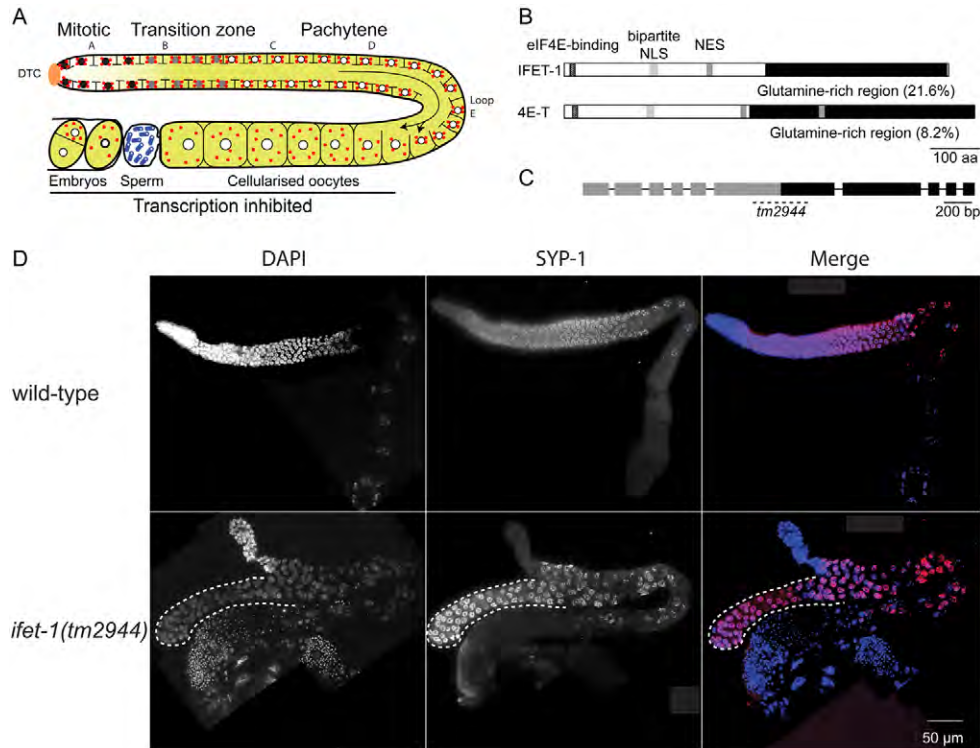
Fig. 1. IFET-1 is a 4E-T required for normal gonad organization in *C. elegans*. (**A**) Illustration of a single hermaphrodite gonad arm. The somatic distal tip cell (DTC) maintains a population of germline stem cells. Germ cells enter into meiosis in the transition zone and progress through pachytene, diplotene and arrest in diakinesis. Oocytes are ovulated, fertilized by sperm and begin embryogenesis in the uterus. In most of the gonad, germ cells are only partially enclosed by a membrane and share a common cytoplasmic core that is actively transported into the developing oocytes (indicated by the arrow). P granules (red) associate with nuclei for most of oogenesis, before they detach and become distributed throughout the cytoplasm of the oocyte. CGH-1 and CAR-1 protein expression (highlighted in olive) is low at the distal end of the gonad and dramatically increases from the transition zone forward. The alphabetical zones used to score GFP expression in Table 2 are indicated. (**B**) IFET-1 has a similar domain organization to human 4E-T. Nuclear localization signal, NLS; Nuclear export signal, NES. (**C**) Genomic organization of *ifet-1* and location of the deletion in the *tm2944* mutant. (**D**) Defects associated with loss of IFET-1 at 25°C. In wild-type gonads, SYP-1 staining is evident once germ cells enter the transition zone and continue until late diakinesis. In *ifet-1(tm2944)*, SYP-1 is detected in the transition zone and in part of the bifurcated gonad arm and continues past the loop region. In the proximal gonad, abundant DAPI foci are detected. Loss of SYP-1 signal in *ifet-1* mutant gonads varies throughout nuclei located in what corresponds to the diakinesis region in the wild type, suggesting an apparent disorganization of meiotic progression in this region.

2005). Interestingly, 4E-T homologs are also important regulatory factors during oogenesis in many species. In *Drosophila*, the 4E-T homolog CUP is important for oogenesis where it is required for translational repression and localization of *nanos* and *oskar* mRNAs (Wilhelm et al., 2003; Nakamura et al., 2004; Nelson et al., 2004; Zappavigna et al., 2004), as well as deadenylation of mRNAs (Igreja and Izaurralde, 2011). *Xenopus* 4E-T is expressed in early stage oocytes, interacts with an ovary-specific eIF4E and regulates translation in *in vitro* assays (Minshall et al., 2007). Mouse 4E-T homolog, Clast4, is also highly expressed during oogenesis, however, its role is less well defined (Villaescusa et al., 2006). The *C. elegans* homolog of 4E-T, IFET-1 (previously known as SPN-2/PQN-45), was recently shown to be required for translational regulation of *zif-1* and *mei-1* mRNAs during oocyte maturation and in one-cell stage embryos, respectively (Li et al., 2009; Guven-Ozkan et al., 2010). The function of IFET-1 in the earlier stages of oogenesis in *C. elegans* is unknown.

Here we report that IFET-1 is a broad scale translational repressor of germ cell mRNAs in the distal region of the gonad and is required for normal gonad development and P granule formation. Ultrastructural studies indicate that IFET-1 is required for formation of the electron dense crest and base of P granules that are thought to be sites of mRNA concentration (Schisa et al., 2001; Sheth et al., 2010). Our data support a model in which IFET-1 is required for retention of mRNAs in P granules which allows translational repressor proteins to bind the mRNA prior to export into the core of the gonad.

Results

IFET-1 is required for normal gonad development

IFET-1 (F56F3.1) has ~47% similarity at the amino acid level to human 4E-T and shares the gross overall protein structure, including predicted nuclear import and export signals, a glutamine-rich region in the C-terminus and an eIF4E-binding motif at the N-terminus (Fig. 1B). Microarray analyses indicate *ifet-1* is oogenesis-enriched (Reinke et al., 2004), and it is required for oocyte maturation and early embryonic development (Li et al., 2009; Guven-Ozkan et al., 2010). In mammalian somatic cells, 4E-T is required for P body formation and localization of the CGH-1 ortholog RCK/p54 (Andrei et al., 2005; Ferraiuolo et al., 2005). To examine if 4E-T is important

for perinuclear P granule formation we obtained the previously uncharacterized deletion mutant *ifet-1(tm2944)* (Fig. 1C), which appears to be a strong loss-of-function. Male *ifet-1(tm2944)* animals are fertile (data not shown), however, *ifet-1(tm2944)* hermaphrodites are sterile, indicating that IFET-1 has a major role in oogenesis. Gonads lacking IFET-1 appeared grossly normal in size, however, the distal region had a bulbous shape, similar to what has been described for animals lacking CGH-1 (Table 1; supplementary material Fig. S1) (Navarro et al., 2001). When grown at 20°C, *ifet-1(tm2944)* gonads displayed a mildly disorganized meiotic progression and contained a mixture of oocytes in diakinesis and pachytene stages in the proximal gonad (supplementary material Figs S2, S3). When grown at 25°C an unusual phenotype observed in ~14% of animals was a bifurcation of the gonad shortly after the transition zone (Fig. 1D; Table 1). The bifurcated arm lacked a distal tip cell, but immunostained positively for the pachytene stage marker SYP-1, a component of the central region of the synaptonemal complex, indicating these cells were at the pachytene stage of meiosis (Fig. 1D). A large number of bright small DAPI staining foci in the proximal region of the gonad (Fig. 1D) stained positively with the sperm-specific antibody SP56 (Table 1; supplementary material Fig. S1B), indicating that these animals had a strong masculinization of the germline (MOG) phenotype: 48% of *ifet-1(tm2944)* hermaphrodites had a mixture of sperm and oocytes in the proximal gonad, while 25% contained only sperm. The switch from sperm to oocyte production in the gonad is highly dependent on post-transcriptional gene regulation (Ellis, 2008). Therefore we investigated if the general translational regulators CGH-1, CAR-1 and PATR-1 synthetically enhanced the MOG phenotype. Knockdown of *cgh-1* in a wild-type background does not induce a MOG phenotype, however in the *ifet-1(tm2944)* background it resulted in a dramatic masculinization of the gonad with 97% of gonads containing only sperm in the proximal gonad (Table 1). Similarly, knockdown of either *car-1* or *patr-1* in the *ifet-1(tm2944)* background resulted in 68% and 52% of gonads, respectively, containing only sperm in the proximal gonad (Table 1). RNAi knockdown of *cgh-1/car-1*, *cgh-1/patr-1* and *car-1/patr-1* did not lead to a MOG phenotype (data not shown, Audhya et al., 2005; Boag et al., 2005). These data suggest that IFET-1 is a key regulator of germline development, likely as a 'general' cap-dependent translational inhibitor that interacts with additional translational inhibitors CGH-1, CAR-1 and PATR-1, reminiscent of the proposed mechanism for decapping mediated mRNA turnover (Nissan et al., 2010).

IFET-1 is required for CGH-1 and CAR-1 to localize to P granules

To further investigate the interactions between IFET-1 and CGH-1/CAR-1 it was important to determine their distributions in the gonad and early embryo. We generated an antibody that specifically recognizes IFET-1 and immunostained 1-day-old adult hermaphrodite gonads (supplementary material Fig. S1A). IFET-1 levels were low in the distal gonad, dramatically increased as germ cells entered meiosis, and remained high throughout the remainder of the gonad, a staining pattern very similar to CGH-1 and CAR-1 (Navarro et al., 2001; Boag et al., 2005). IFET-1 colocalized with the majority of CGH-1/CAR-1 perinuclear P granules throughout the gonad (Fig. 2, data not shown). In the gonad, core IFET-1 was also abundant, with the majority of IFET-1 colocalized with CGH-1 in small foci (Fig. 2). During embryonic development IFET-1 again showed a remarkably similar staining pattern as CGH-1 and CAR-1. In one-cell embryos, IFET-1 was highly expressed and diffusely distributed throughout the cytoplasm and associated with P granules (Fig. 3A). IFET-1 was asymmetrically distributed in the embryo and was significantly enriched in the germ cell lineage (P cells) where it localized to P granules throughout embryogenesis. In the somatic cells of the embryo, IFET-1 abundance was dramatically reduced after the four-cell stage; however, small foci that colocalized with CGH-1 and CAR-1 were evident (Fig. 3A,B) and correspond to P bodies associated with decapping mediated mRNA turnover (Boag et al., 2008).

To test if IFET-1 was required for CGH-1 and CAR-1 localization we immunostained extruded gonads from 1-day-old *ifet-1(tm2944)* animals. Strikingly, both CGH-1 and CAR-1 failed to localize to perinuclear P granules in the absence of IFET-1 and were instead diffusely distributed throughout the gonad (Fig. 4A). Interestingly, in gonads lacking CGH-1, IFET-1 typically failed to localize to perinuclear P granules and was diffusely distributed throughout the gonad, while CAR-1 localized to sheet-like structures in the gonad core (Audhya et al., 2005; Boag et al., 2005). IFET-1 localized to P granules in less than 5% of germ cells (Fig. 4B). To examine if IFET-1 was required for the localization of other perinuclear P granule components, we investigated the localization of two constitutive components, the germ cell-specific proteins PGL-1 and GLH-1. The absence of IFET-1 had little effect on localization of GLH-1, but interestingly PGL-1 localization was severely affected (Fig. 4C). In 60% of *ifet-1(tm2944)* gonads PGL-1 failed to localize to perinuclear P granules, and was instead detected in small foci unassociated with the germ cells (Fig. 4C). The level

Table 1. Defects in *ifet-1(tm2944)* grown at 25°C

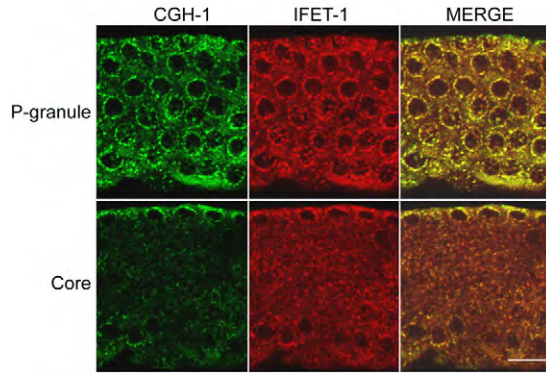| Genotype	Sp (%)	Sp + Oo (%)	Oo (%)	Bulbous (%)	Bifurcation (%)	*n*
Wild type	0	0	100	0	0	33
ifet-1(tm2944)	25	48	27	97	14	77
cgh-1(RNAi)	0	3	97	99	0	69
ifet-1(tm2944); cgh-1(RNAi)	97	2	1	90	4	116
car-1(RNAi)	0	0	100	44	0	41
ifet-1(tm2944); car-1(RNAi)	68	27	5	34	5	44
patr-1(RNAi)	0	0	100	0	0	10
ifet-1(tm2944); patr-1(RNAi)	52	48	0	57	9	21

Sp, sperm; Oo, oocytes.

Fig. 2. IFET-1 colocalizes with CGH-1 in perinuclear P granules and in the gonad core. Pachytene region of extruded gonads from 1-day-old adult hermaphrodites stained for IFET-1 and CGH-1. IFET-1 and CGH-1 colocalize to perinuclear P granules and in abundant foci in the gonad core. Images are projections of three confocal cross-sections through the gonad periphery or core. Scale bar: 5 μm.

of PGL-1 was the same as in wild-type and *ifet-1(tm2944)* adult hermaphrodites (supplementary material Fig. S5A).

With the clear genetic and cell biological interaction uncovered between IFET-1 and CGH-1/CAR-1 in germ cell differentiation, we next asked if the proteins physically interact. We immunoprecipitated endogenous CGH-1 from adult hermaphrodite protein extracts and determined by western blot that IFET-1 co-precipitated. IFET-1 co-immunoprecipitated with CGH-1, but not non-specific IgG control antibody

(supplementary material Fig. S5B). Levels of CGH-1 and CAR-1 were not altered in the absence of IFET-1 (supplementary material Fig. S5A), indicating that the lack of perinuclear P granule localization was not simply due to degradation of these proteins. Together these data suggest that IFET-1 may play a major role in the localization or retention of CGH-1/CAR-1 to perinuclear P granules. Interestingly, IFET-1 has a less dramatic effect on PGL-1 and GLH-1 localization compared to CGH-1 and CAR-1. Previous studies have indicated that the absence of CGH-1 results in defects in PGL-1 localization (Updike and Strome, 2009); therefore, it is possible that the absence of CGH-1 or CAR-1 from perinuclear P granules in *ifet-1(tm2944)* may contribute to the mislocalization of PGL-1.

Ultrastructural analysis of perinuclear P granules

The formation of perinuclear P granules in pachytene germ cells appears to be defective in *ifet-1(tm2944)* worms based on immunocytochemistry data with CAR-1, CGH-1 and PGL-1 (Fig. 4). Therefore we compared the ultrastructure of perinuclear P granules in wild-type and *ifet-1(tm2944)* pachytene stage germ cells by transmission electron microscopy (TEM). P granules were detected as electron dense structures along the nuclear envelope of wild-type and *ifet-1(tm2944)* nuclei. No significant difference was found in the number of perinuclear P granules per nucleus in *ifet-1(tm2944)* compared to wild type ($n=128$ and 153 P granules, respectively). Although variation in the size and shape of P granules was noted, no significant differences in the gross length or height of P granules were detected (Fig. 5). The pachytene nuclei are normally transcriptionally active, and clusters of nuclear pores are organized beneath the P granules,
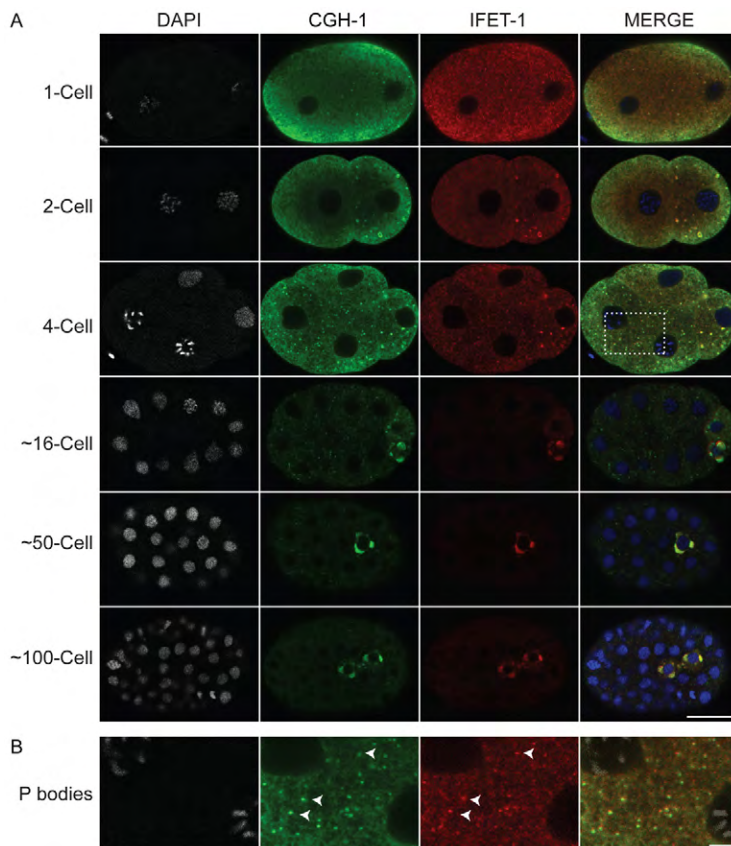

Fig. 3. IFET-1 colocalizes with CGH-1 in the embryo. (**A**) IFET-1 and CGH-1 are concentrated in P granules. Embryos were immunostained for IFET-1 and CGH-1; DNA was visualized by DAPI staining. Until the four-cell stage, IFET-1 and CGH-1 are present as discrete cytoplasmic foci in the somatic cells as well as in the germ cell precursor. After the four-cell stage, most of the detectable IFET-1 and CGH-1 colocalizes to perinuclear aggregates in the germ line precursor cell. Scale bar: 10 μm. (**B**) Detailed images of somatic P bodies in four-cell embryo, corresponding to the boxed region in A. IFET-1 colocalizes with CGH-1 in P bodies in the somatic cells of the embryo. White arrowheads point to P bodies. In all images, anterior is to the left. Scale bar: 2 μm.
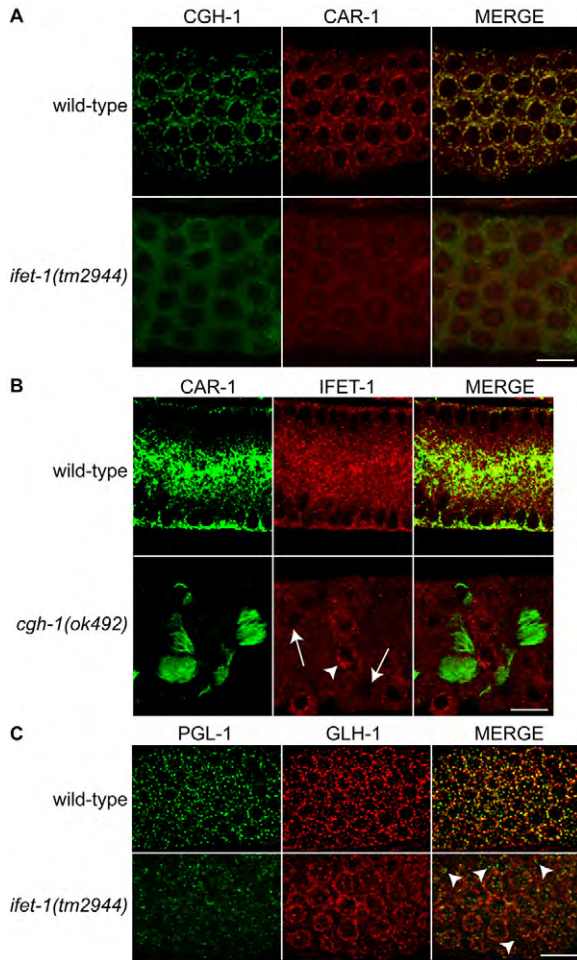
Fig. 4. IFET-1 is required for CGH-1, CAR-1 and PGL-1 localization.
(**A**) Pachytene region of extruded gonads from 1-day-old adult hermaphrodites stained for CGH-1 and CAR-1. In wild-type (N2) gonads, CGH-1 and CAR-1 colocalize to perinuclear P granules. In the absence of IFET-1, CGH-1 and CAR-1 fail to localize to perinuclear P granules and are diffusely distributed throughout the gonad. (**B**) Pachytene region of extruded gonads from 1-day-old adult wild-type and *cgh-1(ok492)* hermaphrodites that were stained for CAR-1 and IFET-1. In wild-type gonads, CAR-1 and IFET-1 localize to perinuclear P granules and foci in the gonad core. In the absence of CGH-1, CAR-1 forms sheet-like structures in the core of the gonad. IFET-1 does not colocalize with the CAR-1 sheets and is diffusely localized throughout the gonad. Although some IFET-1 localizes to perinuclear P granules (white arrowhead), the majority of IFET-1 fails to localize to perinuclear P granules (white arrows). (**C**) Pachytene region of extruded gonads from 1-day-old adult wild-type and *ifet-1(tm2944)* hermaphrodites that were stained for PGL-1 and GLH-1. PGL-1 and GLH-1 colocalize to perinuclear P granules in wild-type gonads. In the absence of IFET-1, the constitutive P granule component PGL-1 forms small foci (white arrowheads) that are not associated with GLH-1-marked perinuclear P granules. GLH-1 localization is largely unchanged in the absence of IFET-1. Images are projections of three confocal cross-sections through the gonad periphery or core. Scale bars: 5 μm.

Fig. 5. Ultrastructure of *ifet-1(tm2944)* P granules reveals fewer electron dense crests and bases, and fewer nuclear pores. (**A**) Cross-section of a nucleus from the pachytene zone of a wild-type gonad. Electron dense crests (C) and bases (B) are frequently detected within the perinuclear P granules (Pg). (**B**) Cross-section of a nucleus from the pachytene zone of an *ifet-1(tm2944)* gonad. (**A′,B′**) Schematic drawings of the P granules shown in A and B, respectively. Higher magnification views of individual P granules, and corresponding schematic drawings, are shown below. Nuclear pores are often seen clustered beneath wild-type P granules (black arrows). Electron dense crests and bases are detected less frequently in *ifet-1(tm2944)* P granules, and fewer nuclear pores are detected beneath P granules. The irregular contour of the *ifet-1(tm2944)* nuclear membrane is probably due to a preparation or fixation artifact. Because no difference was seen between the total length of nuclear membranes in wild-type and *ifet-1(tm2944)* nuclei, the contour does not affect the quantitative analyses of numbers of P granules per nucleus or numbers of nuclear pores per P granule. Scale bars: 1 μm.

leading to the speculation that newly synthesized and translationally repressed maternal mRNAs may preferentially interact with P granules as they are exported through the clusters of nuclear pores (Pitt et al., 2000; Schisa et al., 2001; Sheth et al., 2010). Since IFET-1 is required to repress the translation of several 3′UTR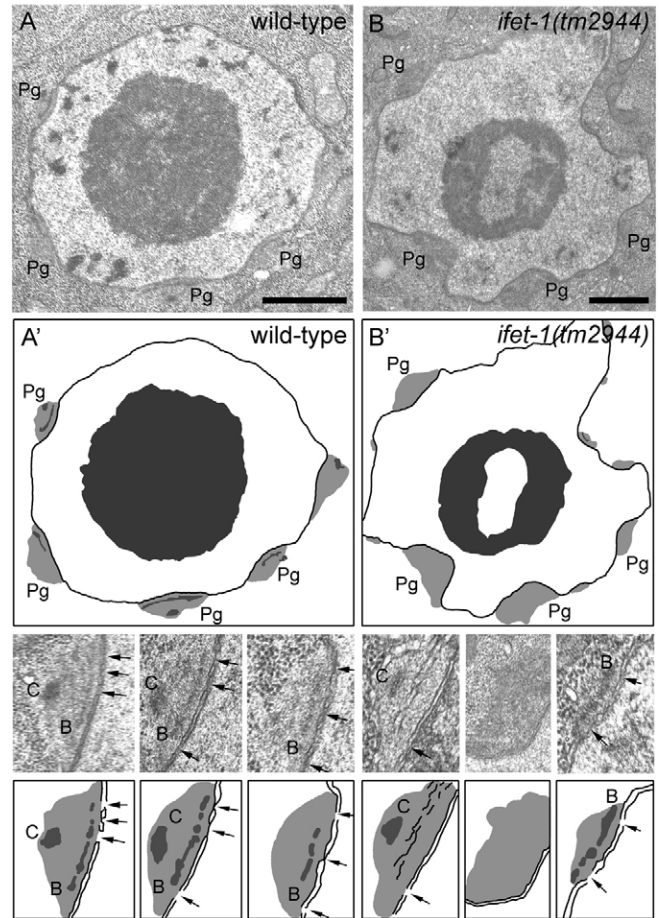 reporter transgenes (Table 2), we were especially interested in any differences in the substructure of P granules that might be consistent with differential levels or trafficking of RNA within *ifet-1(tm2944)* P granules. In the meiotic pachytene nuclei, perinuclear P granules often have an electron-dense 'crest' and 'base' that are ~70–100 nm from the nuclear envelope (Sheth et al., 2010). Both crests and bases appear to decrease in size or disappear once transcription shuts down in diakinesis-stage oocytes, suggesting that the electron dense crests and bases correspond to concentrated mRNA (Sheth et al., 2010). Strikingly we found significantly fewer perinuclear P granules with electron dense bases or crests in *ifet-1(tm2944)* (37%, $n=48$ P granules) compared to wild type (70%, $n=108$ P granules, $P<0.05$)

Table 2. IFET-1 is required for translational regulation of multiple mRNAs

3′UTR	Treatment	Gonad zones				
		A	B	C	D	E
puf-5 (n=100)	control (RNAi)					
	ifet-1(RNAi)					
rme-2 (n=82)	control (RNAi)					
	ifet-1(RNAi)					
lip-1 (n=60)	control (RNAi)					
	ifet-1(RNAi)					
pal-1 (n=80)	control (RNAi)					
	ifet-1(RNAi)					
spn-4 (n=90)	control (RNAi)					
	ifet-1(RNAi)					
mex-3 (n=105)	control (RNAi)					
	ifet-1(RNAi)					
daz-1 (n=58)	control (RNAi)					
	ifet-1(RNAi)					
pie-1 (n=100)	control (RNAi)					
	ifet-1(RNAi)					

Black, high level of GFP expression; dark grey, medium level of GFP expression; light grey, low level of GFP expression. See Fig. 1A for illustration of gonad zones.

(Fig. 5). We next asked if there was any change in the clustering of nuclear pores beneath perinuclear P granules. Interestingly, significantly fewer profiles of nuclear pore complexes were detected beneath *ifet-1(tm2944)* P granules (average of 1.35±0.81 NPCs/P granules) compared to wild-type (average of 2.34±1.26 NPCs/NPCs/P granules, $P<0.05$) (Fig. 5). Overall, these ultrastructural data are consistent with the immunocytochemistry data that indicate structural defects in P granule organization in *ifet-1(tm2944)* hermaphrodite gonads. Despite the absence of several protein components enriched at P granules in *ifet-1(tm2944)*, by TEM the P granules appear similar in shape and size to wild-type P granules. However, the substructure of *ifet-1(tm2944)* P granules does differ significantly from that of wild-type P granules, and the decrease in the number of electron-dense bases, crests, and NPCs beneath P granules is consistent with the model that less maternal mRNA is interacting with the perinuclear P granules.

IFET-1 is required for the translational regulation of multiple mRNAs

In mammalian somatic cells 4E-Ts are thought to act as broad translational inhibitors by disruption of the binding of eIF4G to eIF4E, thereby inhibiting the formation of the pre-initiation complex (Ferraiuolo et al., 2005). To examine if IFET-1 is required for the normal spatial translational regulation of germ cell mRNAs, we used RNAi to knockdown *ifet-1* in eight strains that express a green fluorescent protein (GFP) reporter under the control of different 3′ UTRs (Merritt et al., 2008). RNAi knockdown of *ifet-1* produces gonads with a less severe phenotype compared to the mutant, with the formation of oocytes and the occasional viable progeny produced. Compared to wild-type gonads expressing the reporter genes, *ifet-1(RNAi)* gonads displayed a consistent alteration in GFP localization for each of the GFP-3′UTR strains. In the wild-type background, GFP expressed under the control of the *puf-5*, *rme-2*, *lip-1* or *pal-1* 3′ UTRs were first detected in the late stages of pachytene (zones D/E, see Fig. 1A) and became more abundant as germ

cells entered diplotene and diakinesis (supplementary material Fig. S4) (Merritt et al., 2008). In all four cases, *ifet-1(RNAi)* resulted in GFP expression being detected earlier/more distally in the transition zone (zone B, see Fig. 1A) and extended to the proximal end of the gonad (Table 2; supplementary material Fig. S4). GFP under the control of the *spn-4* or *mex-3* 3′ UTRs had a different expression pattern in wild-type gonads, with expression first detected in the mitotic cells (zones A and B), not seen in the transition zone, pachytene, or diplotene cells (zones B–E), and then detectable in diakinesis stage oocytes. In *ifet-1(RNAi)* gonads, GFP was detectable throughout the gonad (zones A–E). GFP under the control of either the *daz-1* or *pie-1* 3′ UTRs was expressed throughout the gonad in wild-type animals, while in *ifet-1(RNAi)* gonads increased expression levels were detected in the mitotic region (zones A and B, and zones C–D for *daz-1*; Table 2). Interestingly, *puf-5*, *rme-2*, *lip-1*, *pal-1 spn-4* and *mex-3* 3′ UTRs expressed GFP at consistently lower levels in *ifet-1(RNAi)* animals compared to the wild type, suggesting that these mRNAs were either not fully de-repressed, not as efficiently translated, or degraded more rapidly. We were unable to test if knockdown of both *ifet-1* and *cgh-1* in the gonads further released the translational repression of the selected mRNAs as these gonads were highly masculinized (Table 1).

Regulation of poly(A) tail length is an important mechanism to regulate translation, mRNA storage and stability. The *Drosophila* eIF4E-binding protein CUP has recently been shown to play a role in promoting deadenylation of mRNAs (Igreja and Izaurralde, 2011). To test if IFET-1 also plays a role in regulating poly(A) tail length, we selected several predicted cytoplasmic poly(A) polymerase GLD-2 target mRNAs (*egg-1*, *pup-2*, *oma-2* and *pie-1*) (Kim et al., 2010) and assayed their poly(A) tail length in wild type, *gld-2* and *ifet-1(tm2944)* mutants (Fig. 6). As expected, in *gld-2* animals the poly(A) tails were shorter compared to wild-type, reflecting their translational inhibition prior to activation by cytoplasmic adenylation (Fig. 6) (Kim et al., 2010). The distribution of poly(A)-tail lengths was distinctly shorter for each of the GLD-2 target
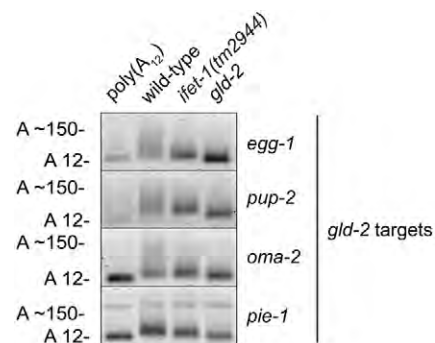

Fig. 6. Analysis of poly(A) tail length in *ifet-1(tm2944)* animals. The poly(A) tail length of four mRNAs in wild-type, *ifet-1(tm2944)* and *gld-2* animals was examined using the ePAT assay (see Materials and Methods). In the wild type, the distribution can extend to ~150 bases. The A~150 and A~12 annotations on the left hand side show the position of the amplicons having poly(A) tails of 12 and 150 residues, respectively. In the absence of the cytoplasmic poly(A)-polymerase GLD-2, all the mRNAs examined had a short poly(A) tail. In the absence of IFET-1, the poly(A) tail length distribution was enriched for shorter poly(A) tails compared with wild type.

mRNAs in *ifet-1(tm2944)* compared to wild-type. The slightly longer size distribution of the poly(A)-tails in *ifet-1(tm2944)* animals is consistent with the interpretation of premature translation and associated deadenylation in transcript aging (Goldstrohm and Wickens, 2008). The size difference in poly(A) tail length between *gld-2* and *ifet-1(tm2944)* animals is consistent with the requirement of CUP for deadenylation and repression of specific mRNAs in *Drosophila* (Igreja and Izaurralde, 2011), suggesting that IFET-1/CUP may function as conserved factors for regulation of poly(A) tail length.

Discussion

In this study we have uncovered a role for the eIF4E-binding protein IFET-1 in gonad development and fertility. In the absence of IFET-1 multiple germ cell reporter mRNAs are prematurely translated, indicating for the first time that IFET-1 functions in early stage germ cells (pachytene). The inhibition of translation is likely mediated by IFET-1 competing with eIF4G to bind eIF4E, thereby inhibiting the formation of the pre-initiation complex. This inhibition appears to use a similar strategy employed by the decapping mediated mRNA turnover in somatic P bodies, where orthologs of CGH-1, CAR-1 and PATR-1 are additional factors required for efficient translational inhibition and mRNA decay. Importantly, we demonstrate that IFET-1 is required for localization of CGH-1 and CAR-1 to perinuclear P granules, and IFET-1 impacts the localization of the constitutive P granule component PGL-1. Interestingly, the substructure of perinuclear P granules is abnormal in the absence of IFET-1 suggesting that RNA transit through the granules may be defective.

IFET-1 is a component of an evolutionarily conserved RNA regulation pathway

In oocytes and neurons an evolutionarily conserved RNA-protein (RNP) complex plays an important role in regulating timing of protein production (Garneau et al., 2007). In *C. elegans*, *D. melanogaster*, *Xenopus* and mouse, this complex regulates translation of specific mRNAs during oogenesis (Paynton, 1998; Nakamura et al., 2001; Navarro et al., 2001; Wilhelm et al., 2003; Nakamura et al., 2004; Boag et al., 2005; Matsumoto et al., 2005; Minshall et al., 2007). Components of the complex include orthologs of the DEAD box RNA helicase CGH-1, Y-box proteins, LSM domain containing proteins, eIF4E and eIF4E-binding proteins. Homology searches indicate that IFET-1 is related to the eIF4E-binding proteins 4E-T and CUP, and it is predicted to perform a similar role in inhibiting cap-dependent translation by competing with eIF4G to bind eIF4E, thereby inhibiting the formation of the pre-initiation complex (Sonenberg and Hinnebusch, 2009). Supporting this model, our data shows the spatial control of translational repression is defective in gonads in which IFET-1 is knocked down, with premature expression of eight mRNAs normally translated only in the proximal region of the gonad (Table 2). Additionally, the poly(A) tails of four out of five mRNAs were intermediate in length compared to wild-type and *gld-2* animals, suggesting that these tails represent the regular shorting of mRNAs during active translation (Goldstrohm and Wickens, 2008).

The pleiotropic phenotypes observed in *ifet-1(tm2944)* hermaphrodites (Fig. 1; supplementary material Fig. S1; Table 1) may be the result of premature translation of multiple mRNAs. The MOG phenotype we identified in *ifet-1(tm2944)* hermaphrodites may reflect defects in post-transcriptional gene regulatory networks upon which the germ cell sex determination pathway is highly dependent (Ellis, 2008). We identified a striking enhancement of the MOG phenotype when the decapping activators *cgh-1*, *car-1* and *patr-1* were knocked down in the *ifet-1(tm2944)* background (Table 1). Interestingly, we were unable to find MOG animals when *cgh-1*, *car-1* or *patr*-1 were knocked down individually or in combination. These data place IFET-1 at the heart of the translational repressive complex that functions early in germ cell development, and are consistent with the predicted function of inhibiting the rate-limiting step of eIF4E-eIF4G binding in cap-dependent translation.

Consistent with previous reports that IFET-1 orthologs are important components of P bodies, we showed that IFET-1 co-localizes with CGH-1 in small foci in somatic cells of the embryo which we have previously identified as P bodies (Fig. 3) (Boag et al., 2008). This suggests that IFET-1 is involved in decapping-mediated mRNA decay in these cells. In *S. cerevisiae*, it has been recently proposed that the first step in mRNA decapping is the inhibition of translation initiation via the combined action of Dhh1, Scd6 and Pat1 (CGH-1, CAR-1 and PATR-1 in *C. elegans*) (Nissan et al., 2010). Our data suggests that a similar mechanism is used to inhibit translational initiation during repression of germ cell mRNAs and for entry of somatic mRNAs into the decapping mediated mRNA turnover pathway.

IFET-1 is required for normal perinuclear P granule formation

An important finding of our studies was the requirement of IFET-1 for CGH-1 and CAR-1 localization to perinuclear P granules. This observation mirrors the requirement of 4E-T for localization of CGH-1/RCK to P bodies in somatic cells (Andrei et al., 2005; Ferraiuolo et al., 2005). An important difference between the perinuclear P granules and P bodies is the origin of the mRNA substrate upon which the protein complex forms. In the case of P bodies, the mRNAs are predominantly derived from a pool of mRNAs that have been translated and were translationally repressed prior to their localization to P bodies (Parker and Sheth, 2007). In the case of perinuclear P granules, the mRNAs are delivered directly to the RNA-granules via the nuclear export machinery. Interestingly, we were unable to detect any significant alteration in GLH-1 localization in the absence of IFET-1, and only incomplete mislocalization of PGL-1, which may also be due to secondary effects related to the lack of CGH-1/CAR-1 (Updike and Strome, 2009).

The failure of CGH-1 and CAR-1 to localize to perinuclear P granules in the absence of IFET-1 suggests that IFET-1 is required either for their transport to perinuclear P granules, or for their retention. IFET-1 homologs 4E-T and CUP are both nucleocytoplasmic shuttling proteins that are important for eIF4E localization. 4E-T is required for the importation of eIF4E into the nucleus (Dostie et al., 2000), while CUP is required for the posterior localization of eIF4E within the cytoplasm of developing oocytes (Zappavigna et al., 2004). Interestingly, in addition to binding the mRNA cap, eIF4Es are able to bind to specific motifs in the 3′ UTR of some mRNAs (Culjkovic et al., 2005; Rong et al., 2008). IFET-1 contains predicted nuclear localization (NLS) and export signals (NES) and may also be required for eIF4E localization. It will be important to test if the predicted NLS/NES are functional in IFET-1 and to identify the domains that determine P granule localization of each of these proteins.

Our ultrastructure studies reveal an important defect in perinuclear P granule substructure. In the absence of IFET-1, perinuclear P granules are generally normal in size and distribution, suggesting that the hydrophobic size exclusion mesh (Updike et al., 2011) of the P granules is not affected, consistent with our GLH-1 immunostaining data. Although the size of P granules is not affected, the substructure is significantly altered, with many perinuclear P granules lacking the electron dense crest and/or base substructures which are thought to correspond to areas of localized RNA-enrichments (Sheth et al., 2010). The absence of these substructures suggests that RNAs are either entering P granules at a decreased rate, or are moving through the perinuclear P granules more rapidly. Interestingly the number of NPCs per perinuclear P granule is significantly reduced in the absence of IFET-1 (1.35 NPCs/P granule compared to 2.34 NPCs/P granule in wild type) and may indicate that the rate of mRNA nuclear export is reduced in the absence of IFET-1.

Proposed model of IFET-1 function

We propose a model in which IFET-1 is required for the retention of a subset of germ cell mRNAs in perinuclear P granules and for establishment of their translational repression. In the absence of IFET-1 and perinuclear P granule localization of CGH-1/CAR-1, many germ cell mRNAs are precociously translated and the electron dense crests and bases of perinuclear P granules are not observed. These data are consistent with mRNAs not being retained in the perinuclear P granules and instead rapidly transiting into the cytoplasm where they are available for translation. IFET-1, CGH-1 and CAR-1 all share similar expression patterns in the gonad, in which expression is low in the mitotic cells and dramatically increases concurrent with the increase in transcription as germ cells enter the transition zone (Navarro et al., 2001; Boag et al., 2005). We believe that IFET-1/CGH-1/CAR-1 functions in these transcriptionally active germ cells to generate a robust translational repression complex on germ cell mRNAs shortly after their export to perinuclear P granules and prior to the mRNP complex being exported into the gonad core (Fig. 7). In this model the IFET-1/CGH-1/CAR-1/PATR-1 repressive complex acts as a general inhibitor of translation through the binding of IFET-1 to eIF4E, thereby repressing cap-dependent translation initiation. CGH-1/CAR-1/PATR-1 likely act as 'activators' of mRNA-protein remodeling; however, the mechanism remains unknown.

An important question that remains to be addressed is how is mRNA specificity achieved? One mechanism is to have sequence-specific mRNA binding proteins bind to or act cooperatively with the general inhibitor complex. In *Drosophila* oocytes, CUP physically binds the RNA-binding protein Bruno and represses translation of oskar mRNA via the binding of Bruno to a specific element in the 3′ UTR of the mRNA (Nakamura et al., 2004). In *C. elegans*, it has recently been shown that IFET-1 binds to the sequence-specific RNA-binding proteins OMA-1/-2 and is required for translational repression of *zif-1* and *mei-1* mRNAs in the proximal gonad and one cell-embryo (Li et al., 2009; Guven-Ozkan et al., 2010). OMA-1/-2 are strongly and exclusively detected in the cellularizing oocytes (Detwiler et al., 2001), a period when transcription is already inhibited. This suggests that the OMA proteins bind mRNAs that are already translationally repressed prior to their loading into the cellularizing oocytes. In *Xenopus* oocytes, two distinct
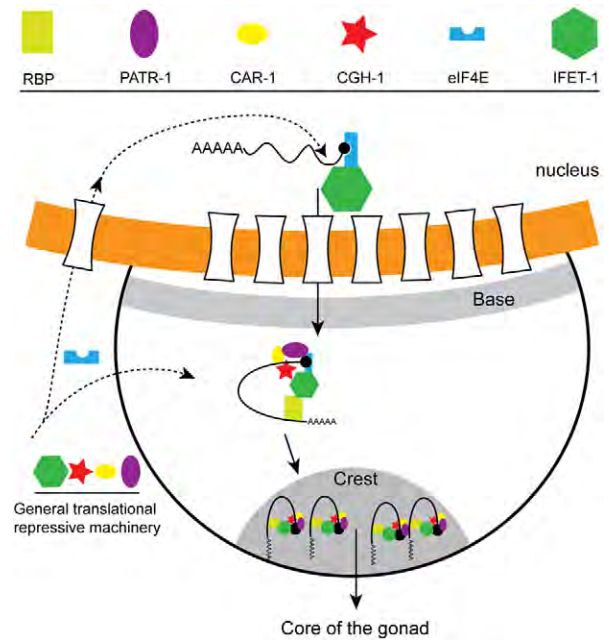

Fig. 7. Proposed model of IFET-1 function. We propose that IFET-1 either recruits or stabilizes the localization of the general translational inhibitors CGH-1, CAR-1 and PATR-1 to P granules. As specific mRNAs exit the nuclear pore they interact with the IFET-1, CGH-1, CAR-1, PATR-1 repressive complex and aggregate at the electron-dense crest and base (both shaded grey) of the P granule. The targeting of specific mRNAs to the repressive complex might be mediated via additional specific RNA-binding proteins. In the absence of IFET-1, CGH-1 and CAR-1 fail to localize to P granules and un-repressed mRNAs exit the P granule environment and are free to be translated by the general translational machinery in the core of the gonad. The movement of un-repressed mRNAs out of the P granules results in the loss of the crest and base substructures of P granules.

translational repressive complexes have been identified. In the early oocyte a large RNP complex containing Xp54 (CGH-1), RAP55B (CAR-1), Pat1 (PATR-1), 4E-T and an ovary-specific eIF4E, repress translation of specific mRNAs (Minshall et al., 2007). In late stage oocytes a second complex is present containing the eIF4E-binding protein Maskin, which increases in abundance at this stage and is important for translational repression and subsequent re-adenylation and translation of specific mRNAs (Cao and Richter, 2002). This suggests that a dynamic two-step mechanism to regulate translation of some germ cell mRNAs by inhibiting the rate-limiting step in formation of the pre-initiation complex is a conserved feature of oogenesis. Given the importance of IFET-1/CGH-1/CAR-1 in mRNA regulation in the gonad, it will be critical to determine how these proteins are trafficked to the perinuclear P granules and the mechanism by which individual mRNAs are identified for translational repression.

Materials and Methods

Strains

Wild-type (N2 Bristol) and mutant strains were maintained using standard methods (Brenner, 1974). The *ifet-1(tm2944)III* deletion mutant was generated by the National BioResource Project for the Nematode and was outcrossed 8 times and balanced using qC1 [dpy-19(e1259) glp-1(q339) qIs26]. Additional strains used were: *cgh-1(ok492)III* and the GFP expressing strains: JH2379 (*pie-1p*:gfp:histone H2B:*pie-1* 3′utr), JH2313 (*pie-1p*:gfp:histone H2B:*rme-2* 3′utr), JH2223 (*pie-1p*:gfp:histone H2B:*daz-1* 3′utr), JH2156 (*pie-1p*:gfp:histone H2B:*lip-1* ORF:*lip-1* 3′utr), JH2311 (*pie-1p*:gfp:histone H2B:*spn-4* 3′utr), JH2013 (*pie-1p*:gfp:*pal-1*

ORF:*pal-1* 3′utr), JH2333 (*pie-1*p:gfp:histone H2B:*mex-3* 3′utr) and JH2418 (*pie-1*p:gfp:: histone H2B:*puf-5* 3′utr) (Merritt et al., 2008).

Antibodies and immunolocalization

Rat affinity-purified polyclonal antibodies were raised against the C-terminal 17 amino acids of IFET-1 [GL Biochem (Shanghai)], Immunostaining with the purified IFET-1 antibody was reduced to background levels in the *ifet-1(tm2944)*. Additional antibodies used were: rabbit anti-CGH-1 (1:300), chicken anti-CAR-1 (1:300) (Boag et al., 2005), monoclonal K76 (1:10) and SP56 (1:300) (Strome and Wood, 1983), chicken anti-GLH-1 (1:200) (Gruidl et al., 1996), guinea pig anti-SYP-1 (1:200), rabbit anti-AIR-2 (1:100), rabbit anti-LAB-1 (1:50), rabbit anti-SMC-3 (1:200), and rabbit anti-HTP-3 (1:200). Species-specific Alexa A488 and A555 (Invitrogen) were used as secondary antibodies, DNA was stained using DAPI and samples were mounted in Dako fluorescent mounting medium. Immunofluorescence images in Figs 2 and 4 were collected using a Zeiss LSM META 510 Confocal microscope. Immunofluorescence images in Figs 1 and 3 and supplementary material Figs S2 and S3 were collected with an IX-71 microscope (Olympus) controlled by the DeltaVision system (Applied Precision). Images were subjected to deconvolution analysis using the SoftWorx 3.0 program (Applied Precision) as in Nabeshima et al. (Nabeshima et al., 2005).

Immunoprecipitation and western blot analysis

Immunoprecipitation of CGH-1 was conducted as described previously (Boag et al., 2005). Western blot analysis of IFET-1 expression was carried out in 50 wild-type and *ifet-1(tm2944)* adult hermaphrodites. The worms were treated with 1×reducing sample buffer and denatured at 95℃ for 5 minutes. Samples were run on 10% SDS-PAGE gels and transferred using standard protocols. The following primary antibodies were used: rat anti-IFET-1 (1:500), chicken anti-CAR-1 (1:500), rabbit anti-CGH-1 (1:500) and mouse monoclonal anti-tubulin DM1A (1:1000; Sigma-Aldrich). Proteins were detected with species-specific HRP-conjugated secondary antibodies goat anti-rat (1:1000; Dako), goat anti-rabbit (1:1000; Dako), rabbit anti-chicken (1:1000; Invitrogen) and goat anti-mouse (1:1000; Invitrogen). Blots were visualized using ECL detection system (GE Healthcare).

RNAi

To analyse the GFP reporter strains, young adult hermaphrodites were injected with double-stranded RNA (1 μg/μl), and allowed to lay eggs for 8 hours before being transferred to new plates. F1 adult hermaphrodites were examined for GFP expression by live imaging. For analysing the MOG phenotype, RNAi was performed by feeding wild-type or *ifet-1(tm2944)* animals from L1 larvae at 25℃ as described previously (Kamath and Ahringer, 2003) and gonads examined 55 hours post L1. pCB19 was used as a control which contains a fragment of *Arabidopsis thaliana* gene with no homology to any known *C. elegans* gene.

Transmission electron microscopy

Adult wild-type and *ifet-1(tm2944)* worms grown at 24℃ were prepared similar to the methods of Pitt et al. (Pitt et al., 2000). Worms were embedded using Spurr's resin, and the worms were oriented for longitudinal sections (Spurr, 1969). Samples were sectioned using a PowerTome×ultramicrotome. Sections were stained with uranyl acetate (saturated) for 25 minutes, rinsed with ddH$_2$O, stained with Reynold's lead citrate for 2 minutes, and rinsed with ddH$_2$O (Reynolds, 1963). Grids were imaged after they dried using a Phillips CM10 transmission electron microscope. Images were captured using Kodak 4489 Electron Microscope Film; negatives were developed with Kodak D19 Developer, fixed with Kodak Professional Rapid Fixer, and rinsed with Kodak Photo Flo, then digitally scanned. The images and plates were formatted and annotated using Adobe Photoshop® CS2. Nuclear membranes were measured by drawing dots on the membrane to sub-divide it into a series of straight lines. Guidelines were placed on each dot, and the measure tool was used to measure from point to point on the nuclear membrane in mm. Measurements in mm were converted to μm (μm=mm/[(total enlargement×magnification)/1000]), where total enlargement is the measurement between two points on the scanned film negative divided by the measurement between the same points on the final image. All statistics were performed using Minitab® 15.

Poly(A) tail length analysis

We used the ePAT approach to examine poly(A) tail length as described in Jänicke et al. (Jänicke et al., 2012). The ePAT method introduces a sequence tag at the 3′ end of adenylated RNA and uses this as an anchor to prime reverse transcription. The combination of gene specific primer and a primer complementary to the tag generates PCR amplicons that vary in their size according to the length of the native poly(A)-tail length distribution. The poly(A$_{12}$) size control indicates the migration of amplicons with an invariant poly(A)-length of 12 residues. Briefly, total RNA was extracted from 100 adult animals and 1 μg of RNA was used in the ePAT reaction. In this approach, a specific sequence tag is added to the 3′ end of adenylated RNA by Klenow polymerase mediated extension. The annealed ePAT oligonucleotide

(5′-GCGAGCTCCGCGGCCGCGTTTTTTTTTTTT-3′) templates the extension of the RNA with dNTPs. For comparison, a poly(A$_{12}$) size control was included. RNA was used in a reverse transcription reaction that uses an anchored primer (5′-GCGAGCTCCGCGGCCGCGTTTTTTTTTTTTVN-3′). The 3′ variable bases lock the primer at the interface between the 3′UTR and the poly(A)-tail for reverse transcription. By this approach an invariant-size PCR product is generated that reflects the size of a short poly(A)-tail of 12 residues. Any additional poly(A)-tail length is visualized as a smear of amplicons of slower migration that extend up (~150 bases) from the size control. The following gene specific primers were used: *pup-2* 5′-CCCACTCTGAACGGATCC-3′; *pie-1*, 5′-CTCTCAGCCACCACCAA-C-3′; *oma-2* 5′-CGTATCCTCTCCCCACACTAAC-3′; *egg-1* 5′-CTCCAAGTT-GACCCTGAACTATTC-3′. PCR amplification was by 28 cycles using using Amplitaq Gold 360 master. The products were resolved on a 2% high-resolution agarose gel and imaged using as previously described using an LAS 3000 imager and Multi Gauge software (Fujifilm).

Bioinformatics

The putative bipartate NLS and NES of IFET-1 were identified using web base tools PSORT II Prediction (Nakai and Horton, 1999) (http://psort.hgc.jp/form2.html) and NetNES 1.1 Server (la Cour et al., 2004) (http://www.cbs.dtu.dk/services/NetNES/).

Author contributions

M.S.S. and P.R.B. conceived and designed the experiments. M.S.S., W.A.L., J.R.P., H.M.K. and T.H.B. performed the experiments. M.S.S., P.R.B., H.M.K., M.P.C., J.R.P., J.A.S., T.H.B. and A.T. analyzed the data. M.S.S. and P.R.B. wrote the paper.

Supplementary material available online at
http://jcs.biologists.org/lookup/suppl/doi:10.1242/jcs.119834/-/DC1

References

Andrei, M. A., Ingelfinger, D., Heintzmann, R., Achsel, T., Rivera-Pomar, R. and Lührmann, R. (2005). A role for eIF4E and eIF4E-transporter in targeting mRNPs to mammalian processing bodies. *RNA* **11**, 717-727.

Audhya, A., Hyndman, F., McLeod, I. X., Maddox, A. S., Yates, J. R., 3rd, Desai, A. and Oegema, K. (2005). A complex containing the Sm protein CAR-1 and the RNA helicase CGH-1 is required for embryonic cytokinesis in Caenorhabditis elegans. *J. Cell Biol.* **171**, 267-279.

Boag, P. R., Nakamura, A. and Blackwell, T. K. (2005). A conserved RNA-protein complex component involved in physiological germline apoptosis regulation in C. elegans. *Development* **132**, 4975-4986.

Boag, P. R., Atalay, A., Robida, S., Reinke, V. and Blackwell, T. K. (2008). Protection of specific maternal messenger RNAs by the P body protein CGH-1 (Dhh1/RCK) during Caenorhabditis elegans oogenesis. *J. Cell Biol.* **182**, 543-557.

Brenner, S. (1974). The genetics of Caenorhabditis elegans. *Genetics* **77**, 71-94.

Cao, Q. and Richter, J. D. (2002). Dissolution of the maskin-eIF4E complex by cytoplasmic polyadenylation and poly(A)-binding protein controls cyclin B1 mRNA translation and oocyte maturation. *EMBO J.* **21**, 3852-3862.

Coller, J. and Parker, R. (2005). General translational repression by activators of mRNA decapping. *Cell* **122**, 875-886.

Culjkovic, B., Topisirovic, I., Skrabanek, L., Ruiz-Gutierrez, M. and Borden, K. L. (2005). eIF4E promotes nuclear export of cyclin D1 mRNAs via an element in the 3′UTR. *J. Cell Biol.* **169**, 245-256.

Detwiler, M. R., Reuben, M., Li, X., Rogers, E. and Lin, R. (2001). Two zinc finger proteins, OMA-1 and OMA-2, are redundantly required for oocyte maturation in C. elegans. *Dev. Cell* **1**, 187-199.

Dostie, J., Ferraiuolo, M., Pause, A., Adam, S. A. and Sonenberg, N. (2000). A novel shuttling protein, 4E-T, mediates the nuclear import of the mRNA 5′ cap-binding protein, eIF4E. *EMBO J.* **19**, 3142-3156.

Ellis, R. E. (2008). Sex determination in the Caenorhabditis elegans germ line. *Curr. Top. Dev. Biol.* **83**, 41-64.

Ferraiuolo, M. A., Basak, S., Dostie, J., Murray, E. L., Schoenberg, D. R. and Sonenberg, N. (2005). A role for the eIF4E-binding protein 4E-T in P-body formation and mRNA decay. *J. Cell Biol.* **170**, 913-924.

Garneau, N. L., Wilusz, J. and Wilusz, C. J. (2007). The highways and byways of mRNA decay. *Nat. Rev. Mol. Cell Biol.* **8**, 113-126.

Goldstrohm, A. C. and Wickens, M. (2008). Multifunctional deadenylase complexes diversify mRNA control. *Nat. Rev. Mol. Cell Biol.* **9**, 337-344.

Gruidl, M. E., Smith, P. A., Kuznicki, K. A., McCrone, J. S., Kirchner, J., Roussell, D. L., Strome, S. and Bennett, K. L. (1996). Multiple potential germ-line helicases are components of the germ-line-specific P granules of Caenorhabditis elegans. *Proc. Natl. Acad. Sci. USA* **93**, 13837-13842.

Guven-Ozkan, T., Robertson, S. M., Nishi, Y. and Lin, R. (2010). zif-1 translational repression defines a second, mutually exclusive OMA function in germline transcriptional repression. *Development* **137**, 3373-3382.

Igreja, C. and Izaurralde, E. (2011). CUP promotes deadenylation and inhibits decapping of mRNA targets. *Genes Dev.* **25**, 1955-1967.

Jänicke, A., Vancuylenberg, J., Boag, P. R., Traven, A. and Beilharz, T. H. (2012). ePAT: a simple method to tag adenylated RNA to measure poly(A)-tail length and other 3′ RACE applications. *RNA* **18**, 1289-1295.

Kamath, R. S. and Ahringer, J. (2003). Genome-wide RNAi screening in Caenorhabditis elegans. *Methods* **30**, 313-321.

Kawasaki, I., Shim, Y. H., Kirchner, J., Kaminker, J., Wood, W. B. and Strome, S. (1998). PGL-1, a predicted RNA-binding component of germ granules, is essential for fertility in C. elegans. *Cell* **94**, 635-645.

Kim, K. W., Wilson, T. L. and Kimble, J. (2010). GLD-2/RNP-8 cytoplasmic poly(A) polymerase is a broad-spectrum regulator of the oogenesis program. *Proc. Natl. Acad. Sci. USA* **107**, 17445-17450.

la Cour, T., Kiemer, L., Mølgaard, A., Gupta, R., Skriver, K. and Brunak, S. (2004). Analysis and prediction of leucine-rich nuclear export signals. *Protein Eng. Des. Sel.* **17**, 527-536.

Li, W., DeBella, L. R., Guven-Ozkan, T., Lin, R. and Rose, L. S. (2009). An eIF4E-binding protein regulates katanin protein levels in C. elegans embryos. *J. Cell Biol.* **187**, 33-42.

Matsumoto, K., Kwon, O. Y., Kim, H. and Akao, Y. (2005). Expression of rck/p54, a DEAD-box RNA helicase, in gametogenesis and early embryogenesis of mice. *Dev. Dyn.* **233**, 1149-1156.

Merritt, C., Rasoloson, D., Ko, D. and Seydoux, G. (2008). 3′ UTRs are the primary regulators of gene expression in the C. elegans germline. *Curr. Biol.* **18**, 1476-1482.

Minshall, N., Reiter, M. H., Weil, D. and Standart, N. (2007). CPEB interacts with an ovary-specific eIF4E and 4E-T in early Xenopus oocytes. *J. Biol. Chem.* **282**, 37389-37401.

Nabeshima, K., Villeneuve, A. M. and Colaiácovo, M. P. (2005). Crossing over is coupled to late meiotic prophase bivalent differentiation through asymmetric disassembly of the SC. *J. Cell Biol.* **168**, 683-689.

Nakai, K. and Horton, P. (1999). PSORT: a program for detecting sorting signals in proteins and predicting their subcellular localization. *Trends Biochem. Sci.* **24**, 34-35.

Nakamura, A., Amikura, R., Hanyu, K. and Kobayashi, S. (2001). Me31B silences translation of oocyte-localizing RNAs through the formation of cytoplasmic RNP complex during Drosophila oogenesis. *Development* **128**, 3233-3242.

Nakamura, A., Sato, K. and Hanyu-Nakamura, K. (2004). Drosophila cup is an eIF4E binding protein that associates with Bruno and regulates oskar mRNA translation in oogenesis. *Dev. Cell* **6**, 69-78.

Navarro, R. E., Shim, E. Y., Kohara, Y., Singson, A. and Blackwell, T. K. (2001). cgh-1, a conserved predicted RNA helicase required for gametogenesis and protection from physiological germline apoptosis in C. elegans. *Development* **128**, 3221-3232.

Nelson, M. R., Leidal, A. M. and Smibert, C. A. (2004). Drosophila Cup is an eIF4E-binding protein that functions in Smaug-mediated translational repression. *EMBO J.* **23**, 150-159.

Nissan, T., Rajyaguru, P., She, M., Song, H. and Parker, R. (2010). Decapping activators in Saccharomyces cerevisiae act by multiple mechanisms. *Mol. Cell* **39**, 773-783.

Parker, R. and Sheth, U. (2007). P bodies and the control of mRNA translation and degradation. *Mol. Cell* **25**, 635-646.

Paynton, B. V. (1998). RNA-binding proteins in mouse oocytes and embryos: expression of genes encoding Y box, DEAD box RNA helicase, and polyA binding proteins. *Dev. Genet.* **23**, 285-298.

Pepling, M. E., Wilhelm, J. E., O'Hara, A. L., Gephardt, G. W. and Spradling, A. C. (2007). Mouse oocytes within germ cell cysts and primordial follicles contain a Balbiani body. *Proc. Natl. Acad. Sci. USA* **104**, 187-192.

Pitt, J. N., Schisa, J. A. and Priess, J. R. (2000). P granules in the germ cells of Caenorhabditis elegans adults are associated with clusters of nuclear pores and contain RNA. *Dev. Biol.* **219**, 315-333.

Reinke, V., Gil, I. S., Ward, S. and Kazmer, K. (2004). Genome-wide germline-enriched and sex-biased expression profiles in Caenorhabditis elegans. *Development* **131**, 311-323.

Reynolds, E. S. (1963). The use of lead citrate at high pH as an electron-opaque stain in electron microscopy. *J. Cell Biol.* **17**, 208-212.

Rong, L., Livingstone, M., Sukarieh, R., Petroulakis, E., Gingras, A. C., Crosby, K., Smith, B., Polakiewicz, R. D., Pelletier, J., Ferraiuolo, M. A. et al. (2008). Control of eIF4E cellular localization by eIF4E-binding proteins, 4E-BPs. *RNA* **14**, 1318-1327.

Schisa, J. A., Pitt, J. N. and Priess, J. R. (2001). Analysis of RNA associated with P granules in germ cells of C. elegans adults. *Development* **128**, 1287-1298.

Sheth, U. and Parker, R. (2003). Decapping and decay of messenger RNA occur in cytoplasmic processing bodies. *Science* **300**, 805-808.

Sheth, U., Pitt, J., Dennis, S. and Priess, J. R. (2010). Perinuclear P granules are the principal sites of mRNA export in adult C. elegans germ cells. *Development* **137**, 1305-1314.

Sonenberg, N. and Hinnebusch, A. G. (2009). Regulation of translation initiation in eukaryotes: mechanisms and biological targets. *Cell* **136**, 731-745.

Spike, C., Meyer, N., Racen, E., Orsborn, A., Kirchner, J., Kuznicki, K., Yee, C., Bennett, K. and Strome, S. (2008). Genetic analysis of the Caenorhabditis elegans GLH family of P-granule proteins. *Genetics* **178**, 1973-1987.

Spurr, A. R. (1969). A low-viscosity epoxy resin embedding medium for electron microscopy. *J. Ultrastruct. Res.* **26**, 31-43.

Strome, S. and Lehmann, R. (2007). Germ versus soma decisions: lessons from flies and worms. *Science* **316**, 392-393.

Strome, S. and Wood, W. B. (1983). Generation of asymmetry and segregation of germ-line granules in early C. elegans embryos. *Cell* **35**, 15-25.

Updike, D. L. and Strome, S. (2009). A genomewide RNAi screen for genes that affect the stability, distribution and function of P granules in Caenorhabditis elegans. *Genetics* **183**, 1397-1419.

Updike, D. L., Hachey, S. J., Kreher, J. and Strome, S. (2011). P granules extend the nuclear pore complex environment in the C. elegans germ line. *J. Cell Biol.* **192**, 939-948.

Villaescusa, J. C., Allard, P., Carminati, E., Kontogiannea, M., Talarico, D., Blasi, F., Farookhi, R. and Verrotti, A. C. (2006). Clast4, the murine homologue of human eIF4E-Transporter, is highly expressed in developing oocytes and post-translationally modified at meiotic maturation. *Gene* **367**, 101-109.

Voronina, E., Seydoux, G., Sassone-Corsi, P. and Nagamori, I. (2011). RNA granules in germ cells. *Cold Spring Harb. Perspect. Biol.* **3**, a002774.

Wilhelm, J. E., Hilton, M., Amos, Q. and Henzel, W. J. (2003). Cup is an eIF4E binding protein required for both the translational repression of oskar and the recruitment of Barentsz. *J. Cell Biol.* **163**, 1197-1204.

Zappavigna, V., Piccioni, F., Villaescusa, J. C. and Verrotti, A. C. (2004). Cup is a nucleocytoplasmic shuttling protein that interacts with the eukaryotic translation initiation factor 4E to modulate Drosophila ovary development. *Proc. Natl. Acad. Sci. USA* **101**, 14800-14805.
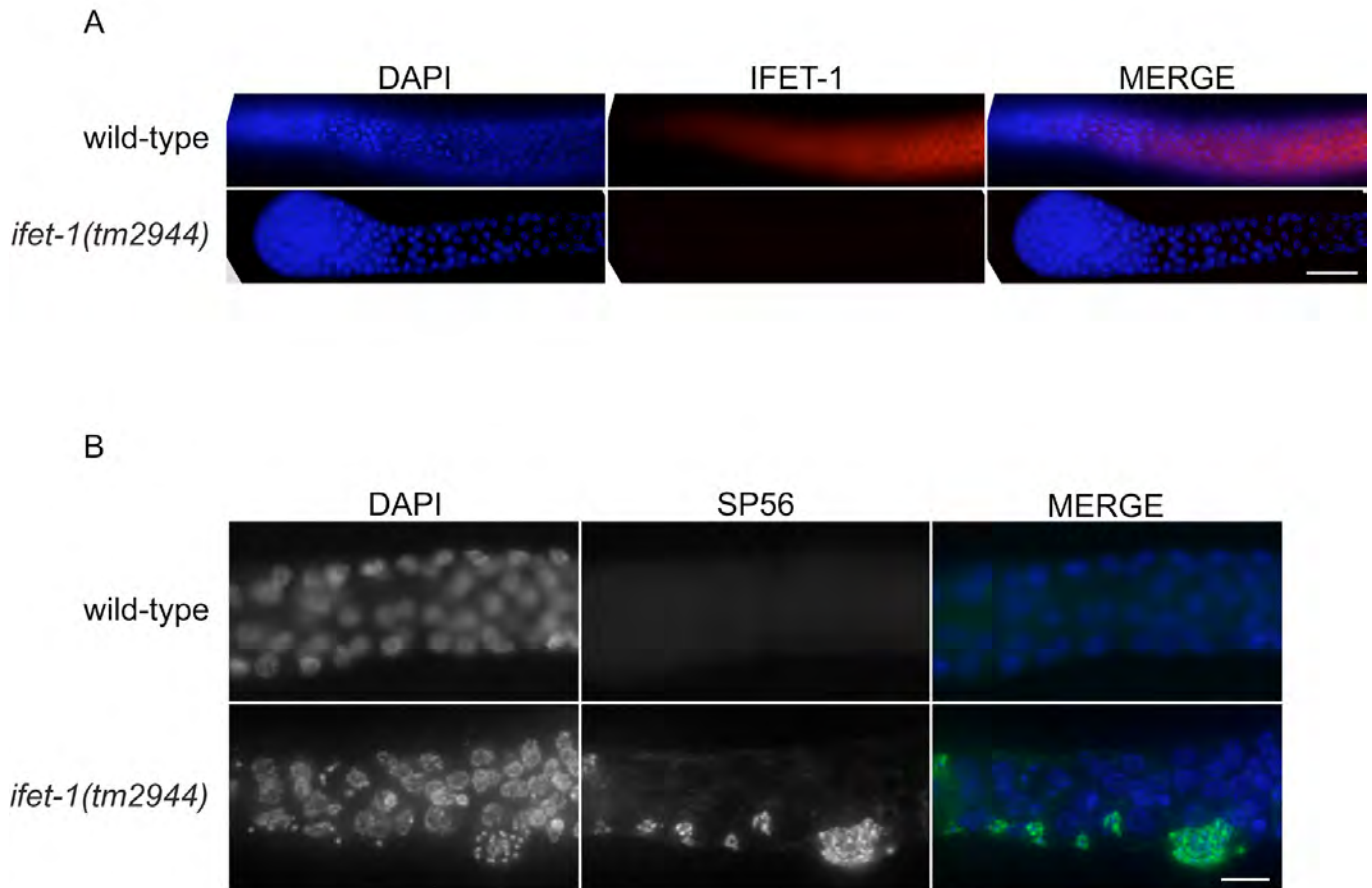
Fig. S1. Immunostaining analysis of *ifet-1(tm2944)* gonads. (A) The anti-IFET-1 antibody specifically recognizes IFET-1. Immunostaining of the distal end of extruded gonads from one-day old adult wild-type and *ifet-1(tm2944)* animals. IFET-1 levels are low at the mitotic region of the distal gonad and increase as germ cells enter the transition zone. No signal above background was detected in the *ifet-1(tm2944)* gonads. The distal region of *ifet-1(tm2944)* gonads displayed a bulbous appearance. Bar represents 20 μm. (B) One-day old *ifet-1(tm2944)* adult hermaphrodites contain sperm in the pachytene region of the gonad. Extruded gonads were immunostained with the sperm-specific antibody SP56 and DNA visualized with DAPI. No SP56 staining is evident in wild-type gonads, while *ifet-1(tm2944)* gonads contain a mixture of SP56 positive and negative cells. Bar represents 10 μm
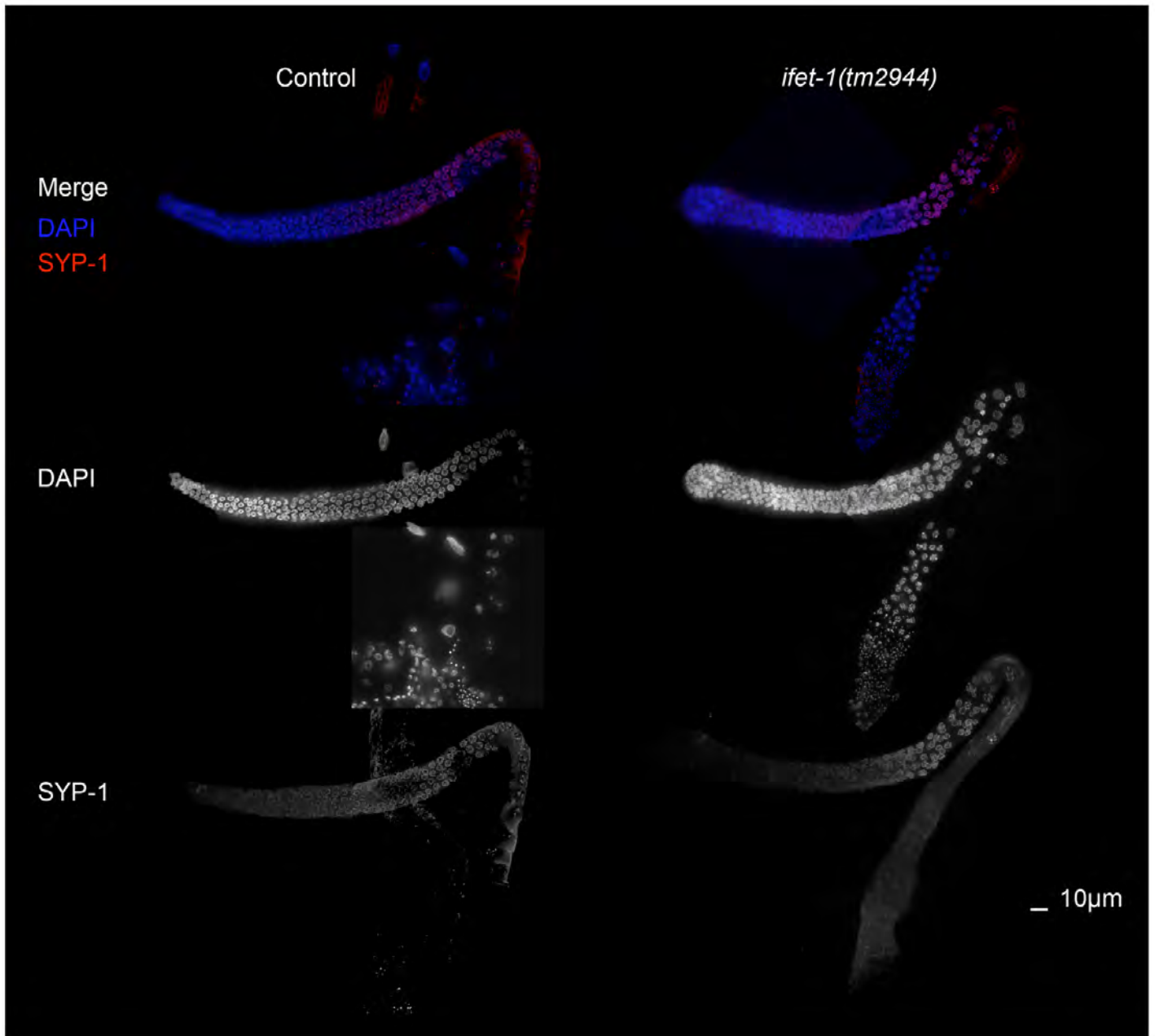
Fig. S2. Disorganization of meiotic progression in *ifet-1(tm2944)* grown at 20ºC. Low magnification images of whole-mount gonads from age-matched wild-type (N2) and *ifet-1(tm2944)* adult hermaphrodites. Analysis of chromosome morphogenesis by examining DAPI-stained chromosomes reveals that *ifet-1(tm2944)* mutants exhibit a disorganized meiotic progression, especially at diakinesis, compared to wild-type. SYP-1 signal is observed associated with chromosomes from transition zone to diakinesis in wild-type gonads. SYP-1 localization upon entry into meiosis is normal in *ifet-1(tm2944)* mutants. However, loss of SYP-1 signal in *ifet-1(tm2944)* gonads varies throughout nuclei located in what corresponds to the diakinesis region in wild-type, suggesting an apparent disorganization of meiotic progression in this region. Bar represents 10 μm.
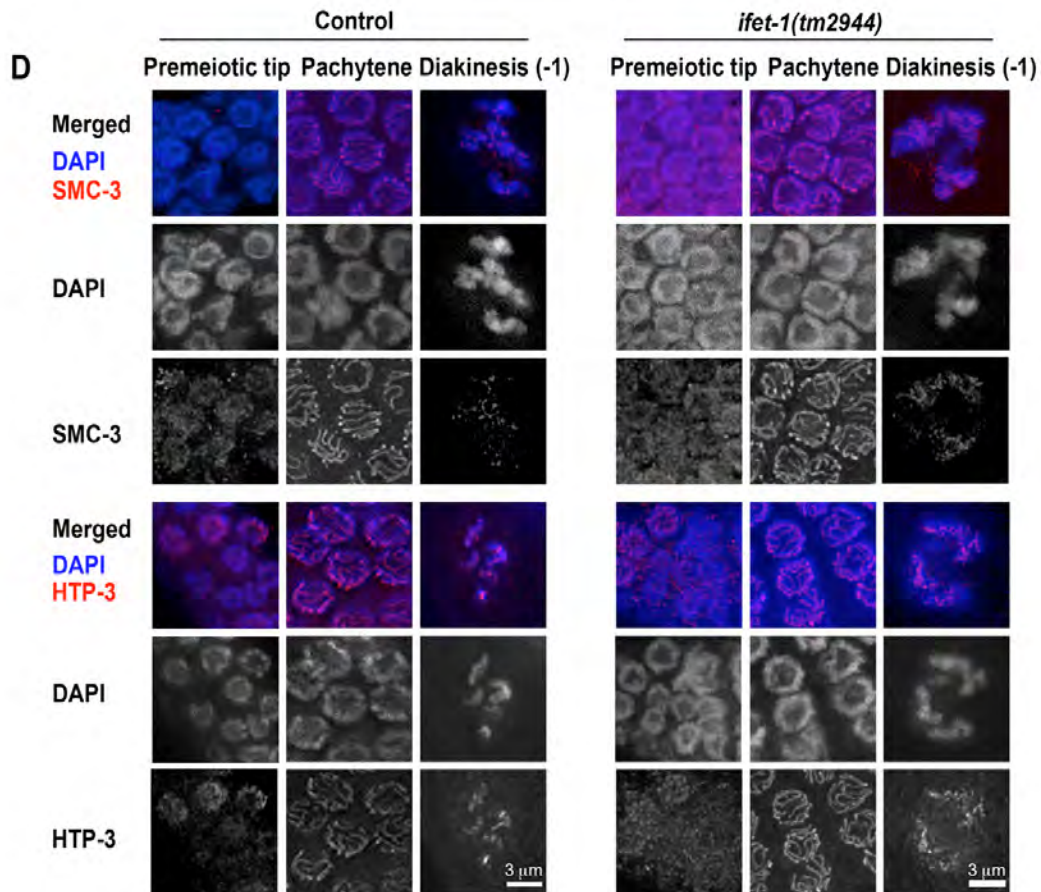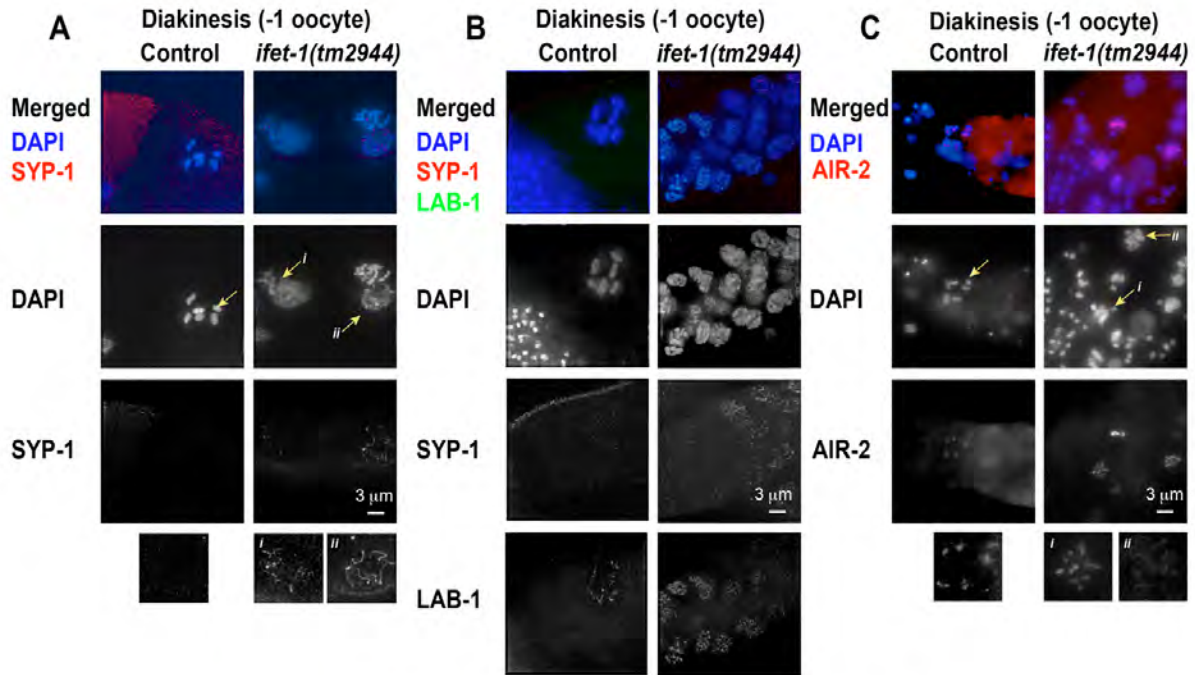
Fig. S3. Analysis of markers of meiotic progression in *ifet-1(tm2944)* grown at 20°C. (A) SYP-1 immunolocalization reveals the presence of mixed-stage meiotic nuclei throughout late prophase in *ifet-1* germlines (27.5%, n=11/40; n= number of gonads examined). Yellow arrows indicate a diakinesis oocyte (*i*) and a pachytene nucleus (*ii*) closely positioned at the end of prophase. (B) SYP-1 and LAB-1 co-immunostaining reveals that in 62.5% (n=25/40) of germlines, nuclei transition normally through late prophase, although they fail to organize into a single row. 10% (n=4/40) of germlines show normal meiotic progression with oocytes acquiring the single file organization characteristic of wild-type upon exit from pachytene (data not shown). (C) AIR-2 immunostaining highlights the presence of late diakinesis oocytes in *ifet-1(tm2944)* gonads. Yellow arrows indicate mixed stages. (D) Immunolocalization of SMC-3 and HTP-3 reveal normal axis morphogenesis throughout meiotic progression in *ifet-1(tm2944)* compared to control.
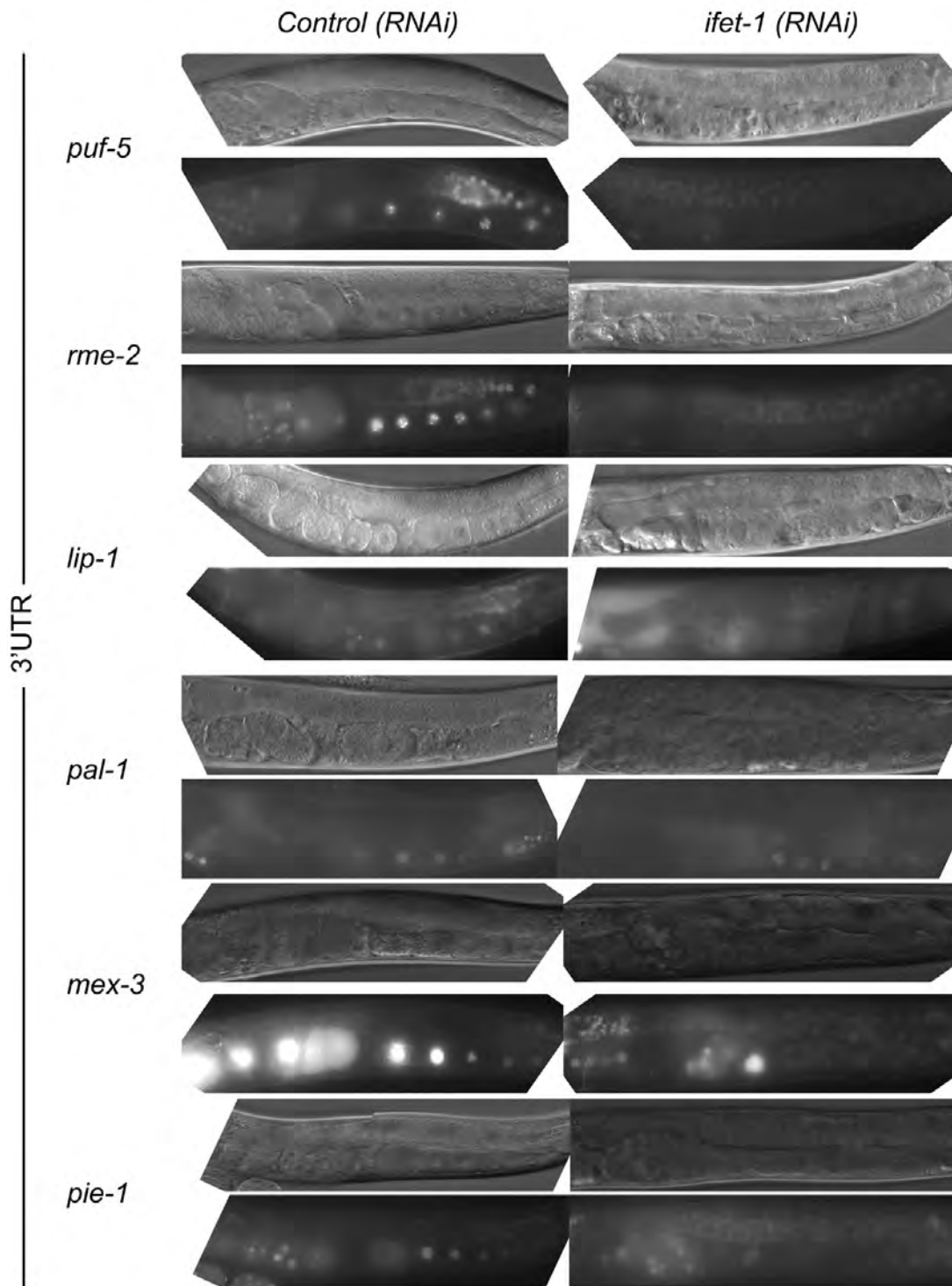
Fig. S4. Derepression of GFP reporter genes in the absence of IFET-1. Representative images of GFP reporter stains that express GFP under the control of specific 3' UTRs. When *ifet-1* was knocked down by RNAi, GFP expression was detected further distally in the gonad.
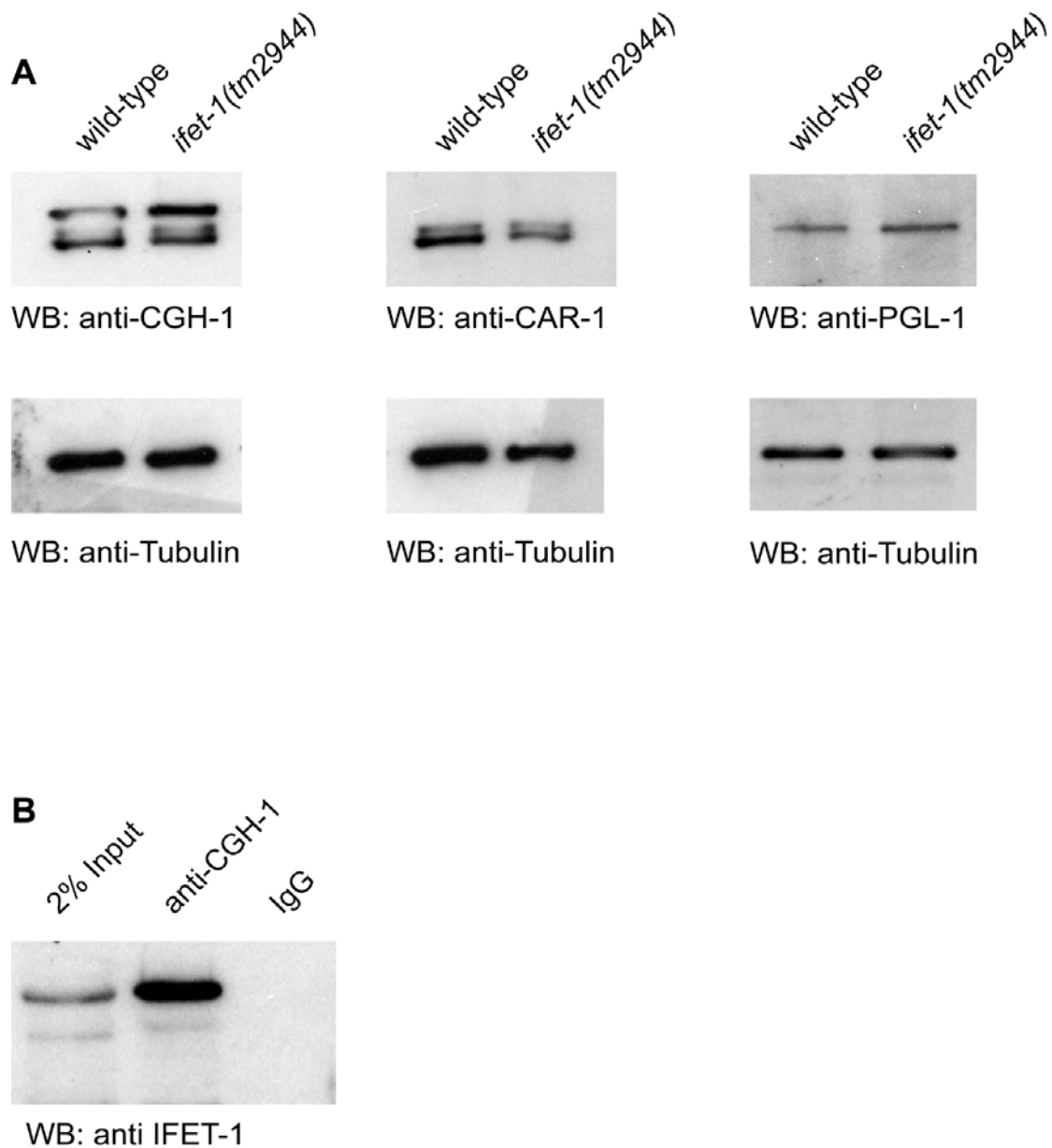
A

wild-type ifet-1(tm2944)

WB: anti-CGH-1

wild-type ifet-1(tm2944)

WB: anti-CAR-1

wild-type ifet-1(tm2944)

WB: anti-PGL-1

WB: anti-Tubulin

WB: anti-Tubulin

WB: anti-Tubulin

B

2% Input anti-CGH-1 IgG

WB: anti IFET-1

Fig. S5. Analysis of IFET-1 interactions with CGH-1 and CAR-1. (A) Western blot analysis of CGH-1, CAR-1 and PGL-1 levels in one-day old adult hermaphrodite animals. Compared to wild-type animals, no change in CGH-1, CAR-1 or PGL-1 levels was detected in the absence of IFET-1. The multiple species of CGH-1 and CAR-1 likely represent alternative phosphorylation states of these proteins. Tubulin was used as a loading control. (B) IFET-1 co-immunoprecipitates with CGH-1 in one-day-old adult hermaphrodites extracts.